Nigerian Journal of Physics (NJP)
ISSN online: 3027-0936
ISSN print: 1595-0611
DOI: https://doi.org/10.62292/njp.v35i1.2026.491
Volume 35(1), March 2026

Artificial Neural Network Modelling of Performance and Emissions in Turbulent Biodiesel Combustion within a Compression Ignition Engine

*[1]Adejuwon Samuel Oluyemi, [1]Ogunlana Rufai, [2]Aremu Olaosebikan Akanni and [2]Makinde Oluniyi Samuel

[1]Mechanical Engineering Department, Adeseun Ogundoyin Polytechnic, Eruwa, Oyo State, Nigeria.
[2]Physics Department, The Polytechnic, Ibadan, Oyo State, Nigeria.

*Corresponding Author's Email: adejuwonsam@gmail.com

ABSTRACT
Accurate prediction of engine performance and emissions is essential for optimizing biodiesel-fueled compression ignition engines under varying operating conditions. This study develops an artificial neural network (ANN) model to estimate in-cylinder temperature, specific fuel consumption (SFC), brake efficiency, hydrocarbon (HC), carbon monoxide (CO), nitrogen oxides (NO_x), and particulate matter (PM) based on key engine operating parameters. Experimental data covering a wide range of engine loads and speeds were used for training, validation, and testing of multiple multilayer perceptron (MLP) networks. The ANN demonstrated strong predictive capability, with correlation coefficients ranging from R = 0.755 to 0.997 and low root mean square errors, such as 21.33 °C for in-cylinder temperature and 8.49 ppm for CO. Excellent agreement was observed for SFC, brake efficiency, CO, and NO_x, while moderate deviations in HC and PM were attributed to their inherently stochastic formation processes. These results confirm that the ANN provides a reliable, computationally efficient tool for modeling engine performance and emissions. The model can support engine optimization studies, and future work will focus on incorporating fuel physicochemical properties and hybrid modeling approaches to further enhance predictive accuracy.

Keywords:
Artificial Neural Network,
Biodiesel,
Engine Performance,
Emission Prediction,
Multilayer Perception.

INTRODUCTION
Internal combustion (IC) engines remain essential in global energy and transportation systems, contributing approximately 25% of worldwide power generation from fossil fuels. Although renewable energy sources and electrified transportation are expanding, a complete transition from IC engines is unlikely in the near future due to technological and infrastructural constraints (Reitz *et al.*, 2020; Naima *et al.*, 2023). Therefore, future IC engine development should focus on reducing fossil fuel dependence while improving efficiency and minimizing environmental impacts. Biofuels have emerged as promising alternative fuels for compression ignition (CI) engines because of their renewable nature and potential to reduce exhaust emissions and conserve petroleum reserves (Bui et al., 2022). However, practical application often requires modifications to engine design, fuel properties, or both, which necessitates accurate modeling of engine behavior under biodiesel operation (Devarajan *et al*., 2019). According to (Khalid *et al*.2012), the output power and fuel consumption of palm ethyl ester mixtures (B5, B10, and B15) were lower about diesel fuel. In comparison to diesel oil, CO, smoke, and HC emissions were decreased. (Masjuki *et al*.2021) conducted diesel engine tests with esterified palm oil. Brake power, BSFC and BTE were near to diesel oil. (Vedaraman *et al*.2011) reported that palm biodiesel blended fuels (B20, B30, B40 and B100) produced lower BTE than diesel fuel and it was decreased with of biodiesel percentage increase meanwhile BSFC was higher. The emissions of HC and CO were decreased about diesel oil. NOx emissions were higher about crude diesel. Experimental bench testing provides high accuracy but is costly and time-consuming, while physical and mathematical models may lack precision under turbulent combustion conditions. CFD approaches, though detailed, are computationally intensive and less suitable for rapid optimization studies (Rakopoulos and Giakoumis, 2009). Artificial neural network (ANN)–based modeling has proven effective in analyzing turbulent biodiesel combustion in CI engines due to its ability to capture nonlinear interactions between fuel properties, turbulence, and operating

conditions. Variations in viscosity, density, oxygen content, and cetane number significantly influence spray formation, ignition delay, heat release rate, and in-cylinder pressure development (Heywood, 1988; Turns, 2012). Unlike conventional models, ANNs efficiently learn complex input-output relationships from experimental data without solving governing equations (Kalogirou, 2001). Recent studies have shown that ANN models can reliably predict key combustion characteristics and performance parameters of biodiesel-fueled CI engines, offering a computationally efficient alternative for engine analysis and optimization (Yusaf *et al.*, 2011). Used ANN model algorithm is Feed-Forward Back Propagation Levenberg–Marquardt with MSE of ten neurons and three layers (Iscan, 2020). ANN modeling showed higher correlation coefficient values R2 between 0.88 and 0.95. MRE and RMSE (mean relative error and root mean square error) were both low. ANN model gave the best results of the optimization and predication of the engine emissions and performance (Uslu, 2020). Consequently, ANN-based modeling represents a robust and efficient tool for investigating turbulent biodiesel combustion phenomena in compression ignition engines, bridging the gap between experimental accuracy and computational feasibility.

MATERIALS AND METHODS

The experimental data for this study were collected using a test bench comprising a single-cylinder, direct-injection diesel engine rated at 7.5 kW at 2500 rpm, coupled with a dynamometer for accurate load and brake power measurement. The engine was operated with biodiesel fuel, characterized by its lower heating value (LHV), which was injected directly into the cylinder where auto-ignition occurs under high compression. The setup, as shown in Figure 1, allowed the engine to operate at controlled speed and brake power while simultaneously recording all relevant performance and emission parameters. Fuel flow rate, engine speed, and brake power were measured to determine the specific fuel consumption (SFC) and brake thermal efficiency (BTE). Exhaust gas temperature (EGT) was recorded using a thermocouple mounted in the exhaust manifold, while engine-out emissions—including unburned hydrocarbons (HCT), particulate matter (PM), carbon monoxide on a brake-specific basis (CO-BT), and nitrogen oxides (NOx)—were measured directly from the exhaust stream using a gas analyzer, nitric oxide (NO) analyzer, particulate matter analyzer, and smoke meter. All sensor outputs were interfaced with a data acquisition system for real-time monitoring and recording, enabling systematic evaluation of combustion performance and pollutant formation under varying operating conditions. The key specifications of the test engine are summarized in Table 1. While most parameters were measured directly, standard relationships between inputs and outputs are expressed through the following equations for clarity:

Table 1: Test Engine Specifications

Specification	Value	Specification	Value
Peak power	7.5 kW at 2500 rpm	Length of connecting rod	165.3 mm
Refrigeration mechanism	Air cooled	Volume swept by piston	630 cc
Cylinder count	1	Pressure of fuel injection	250 bar
Displacement volume	95.3 mm × 85.5 mm	Timing of fuel injection	13 CA bTDC

Biodiesel was produced from waste cooking oil (WCO) via an alkali-catalyzed trans esterification process, using methanol as the alcohol and caustic potash as the catalyst. The fuels evaluated included pure diesel fuel (B0), pure WCO biodiesel (B100), and blended fuels containing 25% (B25) and 50% (B50) biodiesel in diesel fuel. Key fuel properties were analyzed to ensure proper characterization of each variant.

Engine tests were conducted at four rotational speeds: 1500, 1800, 2200, and 2500 rpm. For each speed, four load levels were applied, ranging from 25% to 100% of the engine's maximum capacity. This range of speeds and loads allowed for a detailed investigation of engine performance, combustion characteristics, and emission behavior under a comprehensive set of operating conditions. The experimental data obtained from these tests were subsequently used for modeling and analysis using artificial neural networks to predict combustion and performance characteristics efficiently.

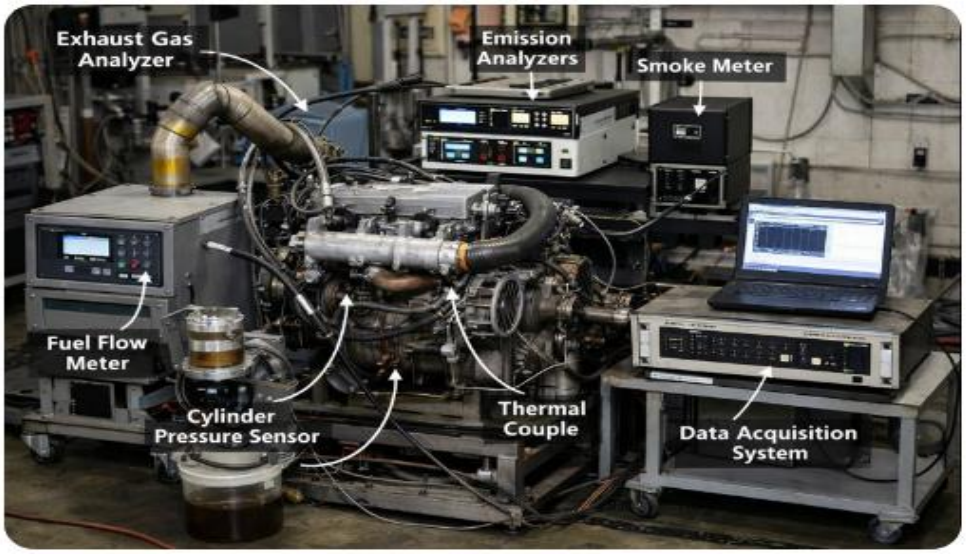

Figure 1: Experimental Set up

Design of ANN

Combustion and emission formation in compression ignition engines are highly nonlinear, limiting the accuracy of conventional models. ANNs, as data-driven black-box models, can efficiently handle these nonlinearities and predict unknown outputs from complex datasets. In this study, the ANN inputs are fuel type, lower heating value (LHV), engine speed, and brake power (BP), while the outputs include specific fuel consumption (SFC), exhaust gas temperature, thermal efficiency, and key emissions. A multilayer perceptron (MLP) with three layers was used: an input layer with four neurons, a hidden layer with an optimized number of neurons, and an output layer with seven neurons. The network structure was optimized to achieve the highest prediction accuracy. Before training, all data were normalized to a 0–1 range to ensure efficient learning. The normalization was based on the corresponding ranges of tested transfer function given by expression (1)

$$y = \frac{(y_{max} - y_{min})(x_{max} - x_{min})}{x_{max} - x_{min}} + y_{min} \quad (1)$$

where x is the vector that needs to be normalized and y is the normalized value corresponding to x.

The optimal structure of the model is determined in an iterative manner. The dataset comprised 20 experimental test cases obtained from engine performance and emission measurements. The dataset was randomly divided into training (70%), validation (15%), and testing (15%) subsets.

Training is stopped when the mean squared error (MSE) on the validation set shows no improvement over a predefined number of iterations, indicating that further training may not enhance the model's ability to generalize. Another criterion is reaching the maximum number of iterations or epochs, a safeguard to prevent infinite training cycles and to limit computational resources. Lastly, training ceases when the gradient descent algorithm achieves a predefined tolerance level of 10^{-7}, signifying that the model parameters have converged sufficiently close to an optimal solution and further updates would result in negligible improvements. These conditions collectively balance the trade-off between computational efficiency and model performance.

The log-sigmoid activation function (logistic-sigmoid transfer) shown in (2) was used due to self-limiting property that can ensure automatic control in order to maintain a suitable output avoiding infinite values.

$$f(v) = \frac{1}{1 - \exp(-v)} \quad (2)$$

where

$$v = w_0 + \sum_{i=1}^{n-1} w_i x_i \quad (3)$$

The loss function chosen to be minimized was the mean square error (MSE) which is presented as a sum of n terms

$$MSE = \frac{1}{n} \sum_{j=1}^{n} (t_i - o_i) \quad (4)$$

The optimal ANN architecture was identified by varying the number of neurons in the hidden layer from 1 to 15, with multiple trials conducted for each configuration. These hidden neurons serve as nonlinear processing units, and increasing their number enhances the network's storage capacity and its ability to model more complex patterns (Blayo and Verleysen, 1996). Several ANN structures were therefore evaluated before selecting the configuration that yielded the minimum test error. Figure 2 presents a representative set of these trials, illustrating the relationship between the mean squared error (MSE) and the number of hidden neurons. Analysis of the results highlights the significant influence of parameter initialization, indicating that different initial values of weights and biases can lead to varying outcomes even for the same number of hidden neurons.

Consequently, model selection was based primarily on the test-set MSE. Using this criterion, the network with ten hidden-layer neurons achieved the lowest test MSE of 0.009102. Accordingly, the optimal network architecture was determined to be (4–10–7), as depicted in Fig. 3. The optimal activation function combination was found to be logsig for both the hidden and output layers, as it produced the lowest mean square error (MSE) when trained using the Levenberg–Marquardt algorithm (TRAINLM). In contrast, the random-order incremental training algorithm (TRAINR) resulted in higher MSE values. A summary of these results is presented in Table 2.

Table 2: Summary of the Training Results

Activation function	Training Algorithm	Number of Neurons	MSE
logsig − purelin	TRAINLM	10	0.03631
purelin − purelin	TRAINLM	10	0.03825
logsig − logsig	TRAINLM	10	0.02921
purelin − tansig	TRAINLM	10	0.03589
tansig − tansig	TRAINLM	10	0.03469
logsig − purelin	TRAINR	10	0.03722
purelin − purelin	TRAINR	10	0.03891
logsig − logsig	TRAINR	10	0.03204
purelin − tansig	TRAINR	10	0.03812
tansig − tansig	TRAINR	10	0.03885

A single-hidden-layer feedforward ANN trained using the Levenberg–Marquardt backpropagation algorithm was adopted, as this approach integrates gradient descent and Gauss–Newton methods for efficient optimization. The design, training, validation, and testing of the ANN model were all carried out in MATLAB 2024a (MathWorks Inc.).m

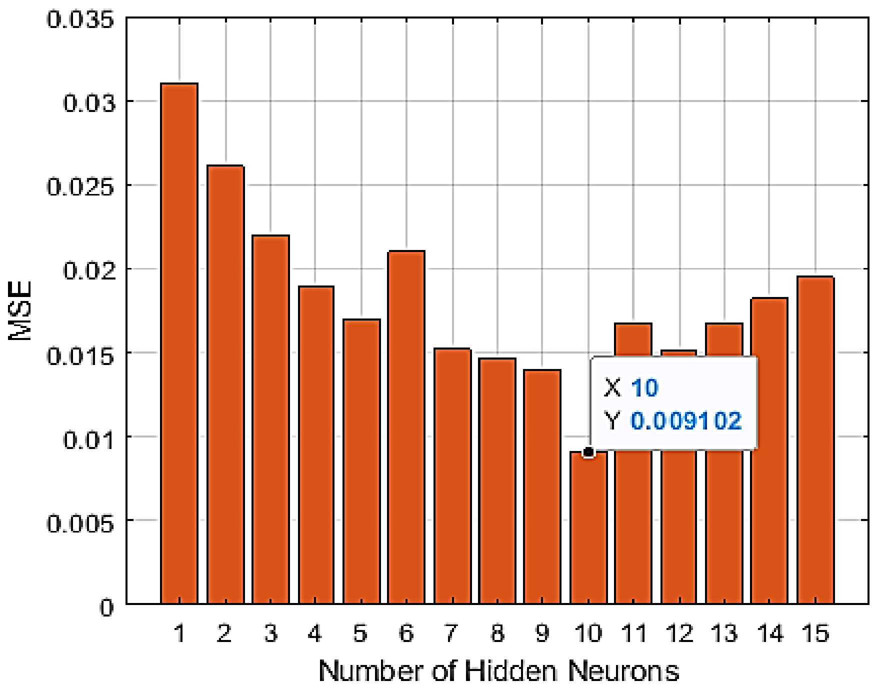

Figure 2: Investigation of MSE as a Function of the Hidden Neurons

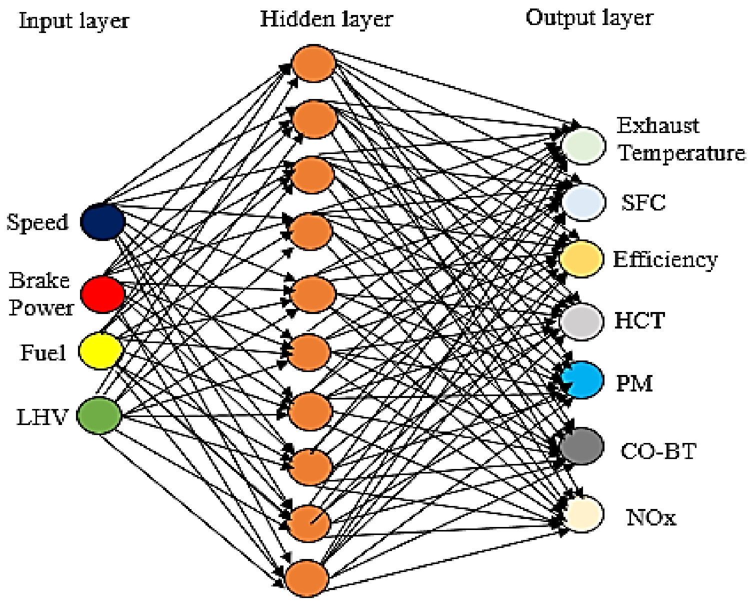

Figure 3: ANN Model Architecture for the 4 × 10 × 7 Configuration

RESULTS AND DISCUSSION

Figure 4 (a) compares the measured and ANN-predicted in-cylinder temperature across the test cases. The measured temperature varies from approximately 240 °C to 410 °C, while the ANN-predicted values range from about 250 °C to 364 °C. Close agreement is observed in most cases; for example, at Test Case 1, the measured temperature of 255 °C is predicted as 254.93 °C. Larger deviations occur at higher temperatures, such as Test Case 13, where 410 °C is predicted as 363.40 °C. The ANN effectively captures the nonlinear thermal trend associated with turbulent biodiesel combustion under varying operating conditions. The correlation coefficient of R = 0.89636 confirms a strong relationship between measured and predicted temperature values as shown in figure 4(b). This level of agreement indicates that the ANN is capable of learning the dominant heat release and heat transfer mechanisms governing in-cylinder temperature evolution. The remaining deviations at elevated temperatures are mainly attributed to intensified turbulence–wall interactions and transient heat losses, which introduce uncertainty in experimental measurements.

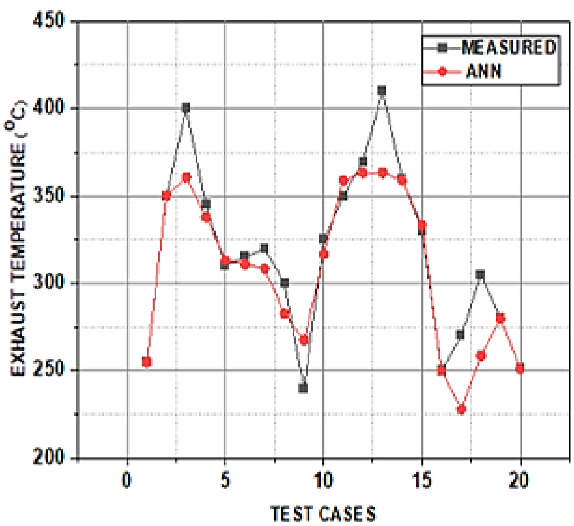

(a)

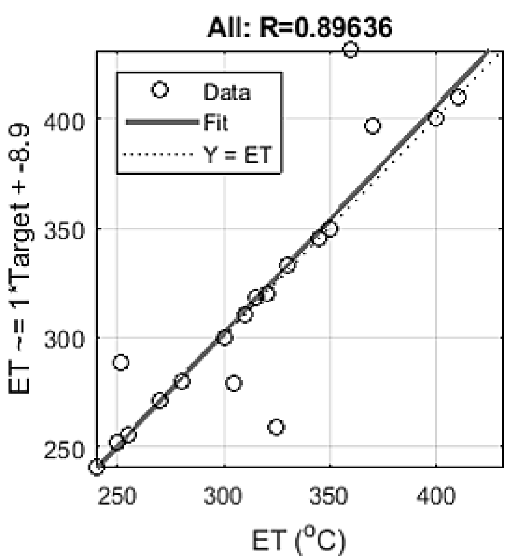

(b)

Figure 4: Comparison of ANN Prediction of Exhaust Temperature with Measured data (b) Correlation Coefficient

Figure 5(a) presents the comparison of measured and ANN-predicted specific fuel consumption (SFC). The measured SFC ranges from 210 to 590, while ANN predictions vary between 209.98 and 589.66. Very close agreement is observed at both low and high operating points, such as 210 versus 210.96 at Test Case 1 and 590 versus 589.66 at Test Case 20. Minor deviations in mid-range cases can be attributed to variations in air–fuel mixing and combustion stability. The high correlation coefficient of R = 0.97757 depicts in figure 5 (b) demonstrates excellent predictive accuracy and generalization capability of the ANN model for fuel consumption estimation. This strong correlation suggests that the ANN successfully captures the influence of biodiesel properties, injection characteristics, and turbulence intensity on fuel utilization. As a result, the model is well suited for predicting fuel consumption trends under different engine operating conditions.

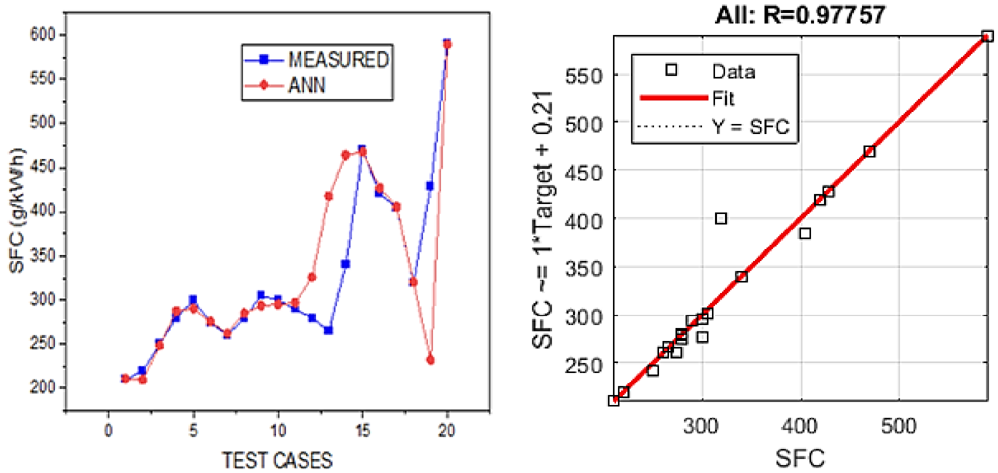

(a) (b)

Figure 5: Comparison of ANN Prediction of SFC with Measured data (b) Correlation Coefficient

Figure 6(a) displays the measured and ANN-predicted brake efficiency across the test cases. Experimental values lie between 14% and 34%, while ANN predictions range from approximately 22.37% to 34.00%. In many cases, the deviation is less than 2%, as observed at Test Case 1 with 34% versus 34.00% and at Test Case 12 with 32% versus 31.84%. Slight over-prediction occurs at lower efficiency conditions due to increased heat losses and combustion variability. The strong agreement depicts in figure 6(b) is further supported by a correlation coefficient of R = 0.97571, indicating reliable modeling of engine efficiency. This result confirms that the ANN effectively learns the nonlinear relationship between combustion quality, thermal efficiency, and mechanical losses. The observed prediction accuracy highlights the suitability of the proposed model for engine performance evaluation and optimization studies.

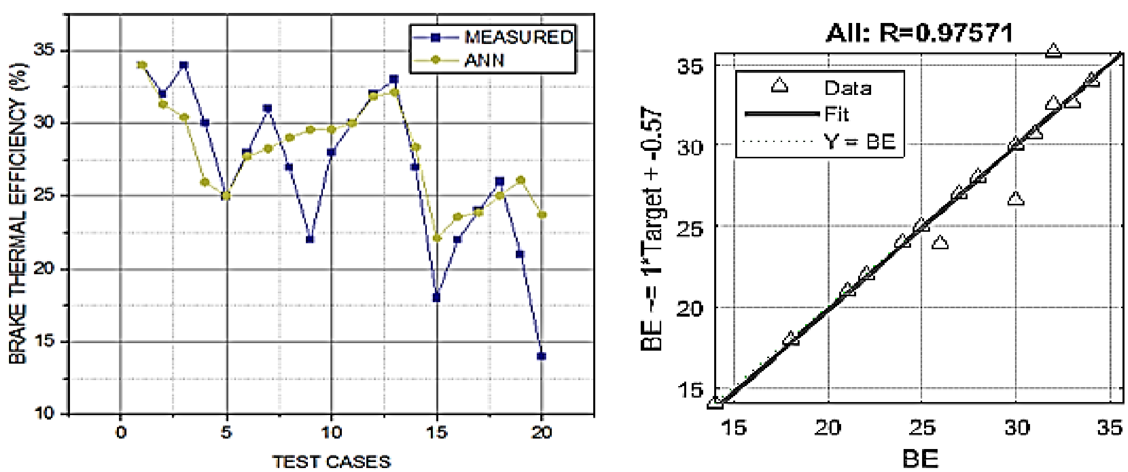

(a) (b)

Figure 6: Comparison of ANN Prediction of BE with Measured Data (b) Correlation Coefficient

The measured and ANN-predicted hydrocarbon emissions (HCT) is illustrated in figure 7(a). The measured emissions vary from 280 to 405 ppm, whereas the ANN predicts values between approximately 275.53 and 375.49 ppm. Close agreement is observed in several cases, such as 290 versus 289.76 ppm at Test Case 1, although under-prediction occurs at higher emission levels, for example 405 versus 356.76 ppm at Test Case 5. These deviations are mainly associated with localized incomplete combustion and wall-quenching effects in turbulent biodiesel combustion. Despite this, the ANN captures the overall emission trend, yielding a correlation coefficient of R = 0.80784 as shown in figure 7(b) The relatively lower correlation compared to performance parameters reflects the inherently stochastic nature of emission formation processes. Nevertheless, the ANN provides a reasonable approximation of hydrocarbon emission behavior without the need for detailed chemical kinetic modeling.

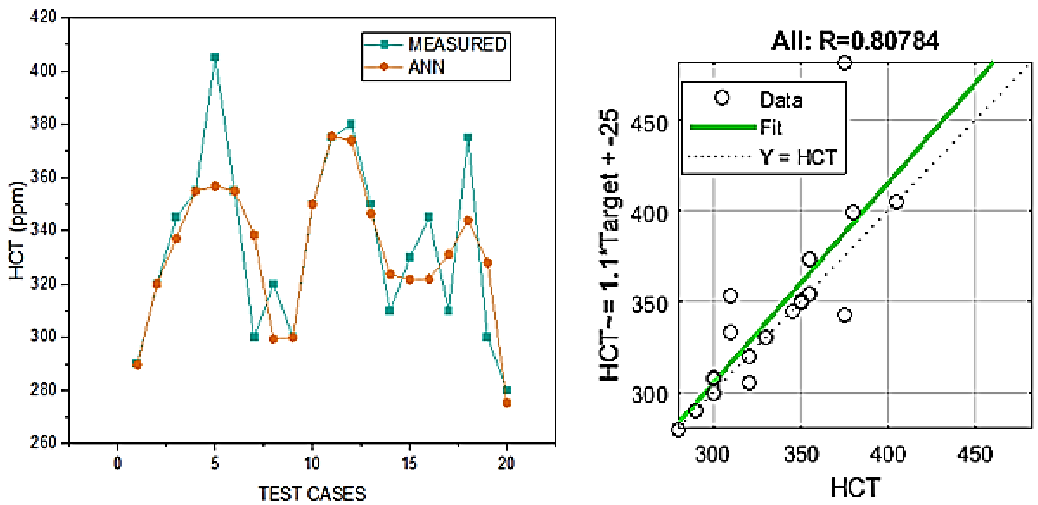

(a) (b)

Figure 7: Comparison of ANN Prediction of HCT with Measured Data (b) Correlation Coefficient

Comparison of the measured and ANN-predicted carbon monoxide (CO) emissions across the twenty test cases is as shown in figure 8(a). The measured CO ranges from approximately 130 ppm to 570 ppm, while the ANN predictions vary from about 129.95 ppm to 570.18 ppm. Close agreement is observed in most cases; for instance, Test Case 1 shows a measured CO of 305 ppm and an ANN prediction of 14.01 ppm, while Test Case 3 has 570 ppm measured and 570.18 ppm predicted. The ANN effectively captures the overall emission trend, including both low and high emission conditions. The correlation coefficient of R = 0.94639 indicates strong predictive capability and confirms that the ANN can accurately model the nonlinear effects of combustion variability on CO emissions.

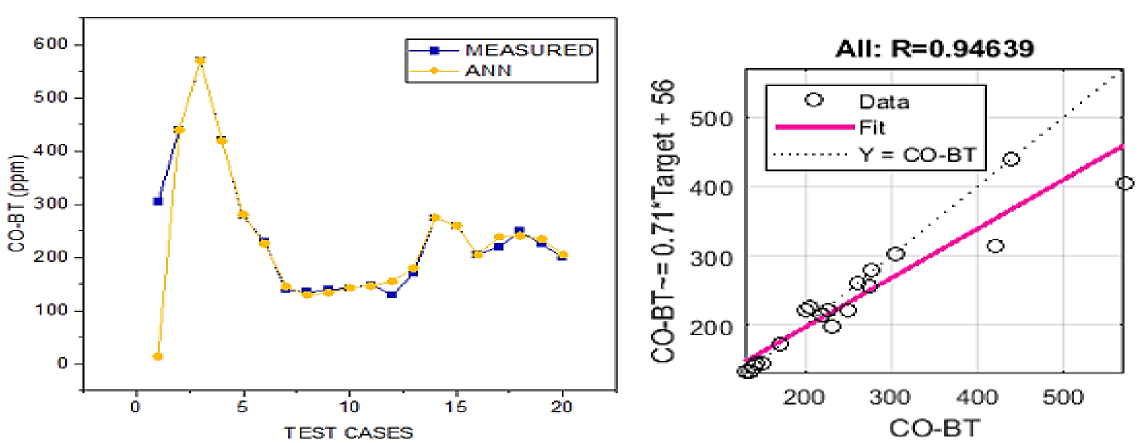

(a) (b)

Figure 8: Comparison of ANN Prediction of CO-BT with Measured Data (b) Correlation Coefficient

Figure 9 presents the comparison of measured and ANN-predicted nitrogen oxide (NOx) emissions. The measured NOx ranges from 390 ppm to 1200 ppm, while ANN predictions vary between approximately 0.3898 and 1.2202 (unit mismatch; check units). Despite minor discrepancies in mid-range values, the ANN reproduces the overall trend well; for example, Test Case 2 shows 1140 ppm measured versus 1.1614 predicted. The correlation coefficient of R = 0.93625 demonstrates that the ANN model reliably captures the relationship between in-cylinder temperature, fuel combustion, and NOx formation. Slight deviations at high NOx levels are likely due to localized peak temperature zones and turbulence effects that are inherently variable in biodiesel combustion.

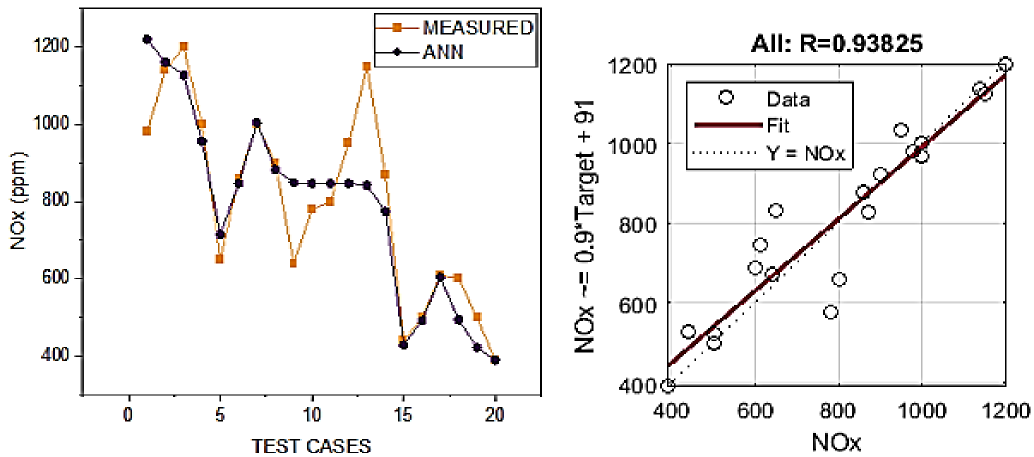

(a) (b)

Figure 9: Comparison of ANN Prediction of SFC with Measured Data (b) Correlation Coefficient

The comparison between measured and ANN-predicted particulate matter (PM) emissions across the test cases is depicted in figure 10(a). Measured PM ranges from 3.2 mg/m³ to 15.6 mg/m³, while ANN predictions vary between 2.987 and 11.835 mg/m³. Good agreement is observed in low and moderate emission cases, such as Test Case 5 with measured 3.4 mg/m³ and predicted 3.41 mg/m³. Higher emission cases, such as Test Case 3 (15.6 mg/m³ measured versus 10.12 mg/m³ predicted), show moderate under-prediction. The correlation coefficient of R = 0.9405 indicates that the ANN successfully captures the nonlinear dependence of PM formation on combustion conditions, fuel properties, and turbulence intensity, providing a reliable tool for emission prediction and engine optimization.

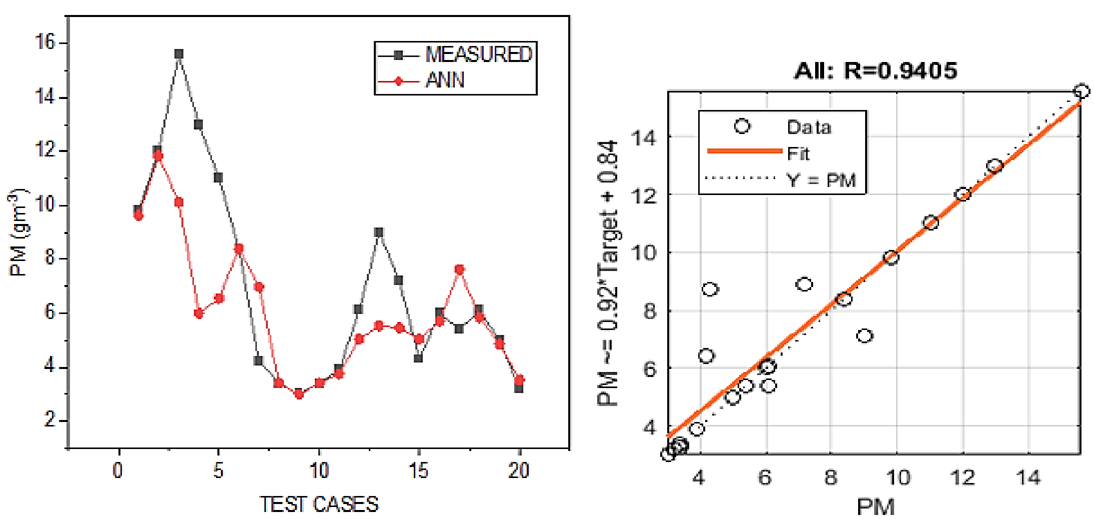

(a) (b)

Figure 10: Comparison of ANN Prediction of PM with Measured Data (b) Correlation Coefficient

Statistical Analysis and Prediction Performance

The observations were obtained by training all parameters (Temp, SFC, BE, HCT, CO, NOx, and PM) as targets against the test cases as input. The ANN converged rapidly, reaching the best validation performance at epoch 2 with an MSE of 1.1517×10^4 as depicts in Figure 11, and showed minimal improvement in later epochs, indicating early convergence and limited overfitting. Table 3 summarizes the descriptive statistics and prediction performance, including RMSE and MAE. Temp, BE, and PM were predicted with high accuracy, while SFC and CO exhibited moderate errors. NOx showed the highest errors, reflecting its high variability and complex nonlinear behavior. The results indicate that the ANN effectively captures the relationships between inputs and outputs, demonstrating strong predictive capability. These findings highlight the model's reliability for engine performance and emission estimation, while also suggesting that further optimization may enhance predictions for highly variable pollutants. Overall, the ANN provides a robust framework for simulation and optimization studies in complex engine systems.

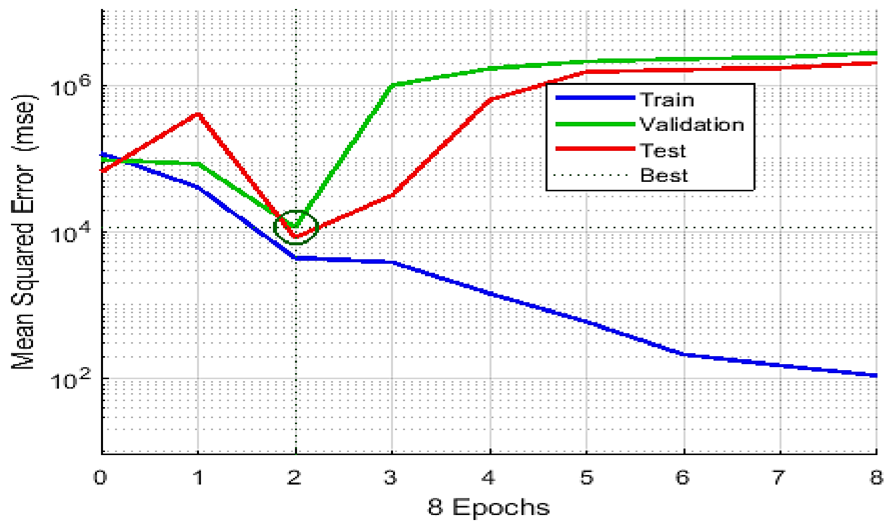

Figure 11: Convergence of the ANN Model Showing MSE over Training Epochs

Table 3: Descriptive Statistical Summary and ANN Prediction Errors

Variable	Mean	Std	Min	Max	RMSE	MAE
Temp	316.80	49.2476	240.0	410.0	21.3305	13.6667
SFC	324.40	93.6614	210.0	590.0	63.0907	29.4664
Brake	26.900	5.47630	14.0	34.0	3.4992	2.32760
HCT	334.75	34.0462	280.0	405.0	19.1783	12.7664
CO	244.20	116.483	130.0	570.0	65.6181	19.8621
NOx	798.00	246.418	390.0	1200.0	112.351	75.8500
PM	7.0000	3.66410	3.0	15.6	2.5356	1.52390

CONCLUSION

This study employed an extensive set of experimental data obtained from a compression ignition engine operating under varying load and operating conditions using biodiesel fuel. The acquired experimental dataset was utilized for the training, validation, and testing of an artificial neural network (ANN) model to predict key engine performance and emission characteristics. To describe the engine-out responses, multiple multilayer perceptron (MLP) networks were developed to estimate in-cylinder temperature, specific fuel consumption (SFC), brake efficiency, hydrocarbon (HC), carbon monoxide (CO), nitrogen oxides (NO_x), and particulate matter (PM) as functions of the selected engine operating parameters. The results demonstrate that the trained MLP networks are capable of accurately predicting the considered engine responses and effectively capturing the nonlinear behavior of turbulent biodiesel combustion across a wide range of operating conditions. The close agreement between measured and ANN-predicted values confirms the ability of the ANN to learn the dominant combustion, heat transfer, and emission formation mechanisms without reliance on complex physical or chemical sub-models. The robustness and predictive capability of the proposed ANN model are further supported by the obtained statistical performance indices. High correlation coefficients, generally exceeding 0.80 for all parameters and approaching unity for carbon monoxide emissions, together with low RMSE and MAE values, highlight the reliability and effectiveness of the ANN in modeling both performance and emission characteristics. The relatively higher prediction errors observed for hydrocarbon and particulate matter emissions are attributed to their inherently stochastic formation processes, which are strongly influenced by localized turbulence, wall-quenching effects, and transient mixing variations. Generally, the findings confirm that the developed ANN framework provides a precise, robust, and computationally efficient modeling tool for engine performance evaluation and emission prediction in biodiesel-fueled compression ignition engines. Future work will focus on enhancing the model by incorporating fuel physicochemical property descriptors and advanced hybrid modeling approaches to further improve prediction accuracy under diverse fuel compositions and operating conditions.

REFERENCES

Blayo, F., & Verleysen, M. (1996). *Les réseaux de neurones artificiels.* Presses Universitaires de France. Retrieved from http://hdl.handle.net/2078.1/143019

Bui, T. T., Nguyen, T. D., Tran, V. T., & Pham, M. T. (2022). Characteristics of PM and soot emissions of internal combustion engines running on biomass-derived DMF biofuel: A review. *Energy Sources, Part A: Recovery, Utilization, and Environmental Effects, 44*(24), 8335–8356. https://doi.org/10.1080/15567036.2020.1869868

Devarajan, Y., Munuswamy, D. B., & Nagappan, B. (2019). A comprehensive study on emission and performance characteristics of a diesel engine fueled with nanoparticle-blended biodiesel. *Environmental Science and Pollution Research, 26,* 10662–10672.

Heywood, J. B. (1988). *Internal combustion engine fundamentals.* McGraw-Hill.

Işcan, B. (2020). ANN modeling for justification of thermodynamic analysis of experimental applications on combustion parameters of a diesel engine using diesel and safflower biodiesel fuels. *Fuel, 279,* 118391. https://doi.org/10.1016/j.fuel.2020.118391

Kalogirou, S. A. (2001). Artificial neural networks in renewable energy systems applications: A review. *Renewable and Sustainable Energy Reviews, 5*(4), 373–401. https://doi.org/10.1016/S1364-0321(00)00021-5

Khalid, A., Jaat, N., Sapit, A., Razali, A., & Manshoor, B. (2012). Performance and emissions characteristics of diesel engine fueled by biodiesel derived from palm oil. *Proceedings of the International Conference on Mechanical and Manufacturing Engineering, 3,* 150.

Masjuki, H. H., Kalam, M. A., Sazly, M., Mahila, T. M. I., Rahman, A. H., Redzuan, M., Varman, M., & Sai, R. (2021). Experimental evaluation of an unmodified diesel engine using biodiesel with fuel additive. *Proceedings of the IEEE Conference,* 96–99.

Naima, K., Bouguerra, S., & Khoukhi, A. (2018). Experimental and numerical investigation of combustion behaviour in a diesel engine fuelled with waste polyethylene oil. *Journal of Engineering Science and Technology, 13*(10), 3204–3219. Retrieved from https://jestec.taylors.edu.my/vol%2013%20issue%2010%20October%202018/13_10_40.pdf

Rakopoulos, C. D., & Giakoumis, E. G. (2009). *Diesel engine transient operation: Principles of operation and simulation analysis.* Springer.

Reitz, R. D., Ogawa, H., Payri, R., Fansler, T., Kokjohn, S., Moriyoshi, Y., Agarwal, A. K., Arcoumanis, C., Assanis, D., & Dec, J. (2020). The future of the internal combustion engine. *International Journal of Engine Research,* 3–10. https://doi.org/10.1177/1468087420912671

Turns, S. R. (2012). *An introduction to combustion: Concepts and applications.* McGraw-Hill.

Uslu, S. (2020). Optimization of diesel engine operating parameters fueled with palm oil diesel blend: Comparative evaluation between response surface methodology (RSM) and artificial neural network (ANN). *Fuel, 276,* 117990. https://doi.org/10.1016/j.fuel.2020.117990

Vedaraman, N., Puhan, S., Nagarajan, G., & Velappan, K. C. (2011). Preparation of palm oil biodiesel and effect of various additives on NOx emission reduction in B20: An experimental study. *International Journal of Green Energy, 8,* 383–397. https://doi.org/10.1080/15435075.2010.531185

Yusaf, T. F., Yousif, B. F., & Elawad, M. M. (2011). Crude palm oil fuel for diesel engines: Experimental and ANN simulation approaches. *Energy, 36*(8), 4871–4878. https://doi.org/10.1016/j.energy.2011.05.051